Multiscale Diagnosis of Mangrove Status in Data-Poor Context Using Very High Spatial Resolution Satellite Images: A Case Study in Pichavaram Mangrove Forest, Tamil Nadu, India

Shuvankar Ghosh, Christophe Proisy, Gowrappan Muthusankar, Hassenrück Christiane, Véronique Helfer, Raphaël Mathevet, Julien Andrieu, Natesan Balachandran, Narendran Rajendran

remote sensing

MDPI

Article

Multiscale Diagnosis of Mangrove Status in Data-Poor Context Using Very High Spatial Resolution Satellite Images: A Case Study in Pichavaram Mangrove Forest, Tamil Nadu, India

Shuvankar Ghosh [1,2], Christophe Proisy [1,3,4,*], Gowrappan Muthusankar [1], Christiane Hassenrück [5,6], Véronique Helfer [5], Raphaël Mathevet [1,7], Julien Andrieu [1,8], Natesan Balachandran [1] and Rajendran Narendran [9]

1 French Institute of Pondicherry, Pondicherry 605001, India; shuvankar.ghosh@ifpindia.org (S.G.); muthusankar@ifpindia.org (G.M.); raphael.mathevet@cefe.cnrs.fr (R.M.); julien.andrieu@ifpindia.org (J.A.); balachandran.n@ifpindia.org (N.B.)
2 Iora Ecological Solutions Pvt. Ltd., New Delhi 110030, India
3 AMAP, University Montpellier, IRD, CNRS, INRAE, 34000 Montpellier, France
4 AMAP, Centre IRD de Cayenne, 97300 Cayenne, France
5 ZMT—Leibniz Centre for Tropical Marine Research, 28359 Bremen, Germany; christiane.hassenrueck@io-warnemuende.de (C.H.); veronique.helfer@leibniz-zmt.de (V.H.)
6 Leibniz Institute for Baltic Sea Research Warnemünde (IOW), 18119 Rostock, Germany
7 CEFE, University Montpellier, CNRS, EPHE, IRD, 34090 Montpellier, France
8 ESPACE, University Cote d'Azur, 06103 Nice, France
9 Centre of Advanced Study in Marine Biology, Faculty of Marine Science, Annamalai University, Parangipettai 608002, India; narenbios666@gmail.com
* Correspondence: christophe.proisy@ird.fr

check for updates

Citation: Ghosh, S.; Proisy, C.; Muthusankar, G.; Hassenrück, C.; Helfer, V.; Mathevet, R.; Andrieu, J.; Balachandran, N.; Narendran, R. Multiscale Diagnosis of Mangrove Status in Data-Poor Context Using Very High Spatial Resolution Satellite Images: A Case Study in Pichavaram Mangrove Forest, Tamil Nadu, India. *Remote Sens.* **2022**, *14*, 2317. https://doi.org/10.3390/rs14102317

Academic Editor: Chandra Giri

Received: 6 April 2022
Accepted: 27 April 2022
Published: 11 May 2022

Publisher's Note: MDPI stays neutral with regard to jurisdictional claims in published maps and institutional affiliations.

Abstract: Highlighting spatiotemporal changes occurring within mangrove habitats at the finest possible scale could contribute fundamental knowledge and data for local sustainable management. This study presents the current situation of the Pichavaram mangrove area, a coastal region of Southeast India prone to both cyclones and reduced freshwater inflow. Based on the supervised classification and visual inspection of very high spatial resolution (VHSR) satellite images provided with a pixel size of <4 m, we generated time-series maps to analyze the changes that occurred in both the natural and planted mangroves between 2003 and 2019. We achieved a high mapping accuracy (>85%), which confirmed the potential of classification techniques applied to VHSR images in capturing changes in mangroves on a very fine scale. Our diagnosis reveals variable expansion rates in plantations made by the local authorities. We also report an ongoing mangrove dieback and confirm progressive shoreline erosion along the coastline. Despite a lack of field data, VHSR images allowed for the multiscale diagnosis of the ecosystem situation, thus constituting the first fine-scale assessment of the fragile Pichavaram mangrove area upon which the coastal community is dependent.

Keywords: remote sensing-based monitoring; plantation; restoration; change detection; dieback; Bay of Bengal

1. Introduction

Each mangrove region has its own history, which reflects how species diversity and structural patterns adapt to local and evolving geomorphic and climatic settings [1,2]. The status of mangroves, however, remains insufficiently documented in many places of the world despite a consensus on their rates of global decline over decadal timescales [3–9]. Even if annual rates of mangrove loss tended to decrease between 2000 and 2012 (0.16–0.39%) compared to the 1980–2000 period (0.99%) [10–14], the present situation in South Asia and Southeast Asia remains illustrative of the major

drivers of global mangrove loss, which include land-use conversion to aquaculture, timber harvesting, pollution, freshwater deficits, low silt deposition, shoreline erosion, and other environmental events, such as dieback, floods, and tropical storm landfalls [8,12,13]. Beyond the awareness of the importance to protect and restore mangroves raised among the public at large including policy makers [13] after the Indian Ocean tsunami in 2004, local and regional administrations must be continuously and at the earliest stage cautioned on the mangrove status for better ecosystem management [15–17].

Mangrove environments are complex forest landscapes where spatiotemporal changes continuously occur at fine spatial scales as a consequence of bio-geomorphological processes operating at different timescales, and the ecosystem transformation remains highly situational. More than anything, progressive small-scale changes occurring within forest landscape area, such as stand structure degradation, dieback, or loss due to sediment erosion, must be monitored to detect stress factors as early as possible [17–19].

As evident from Figure 1, mangrove species distribution, forest structural attributes, or landscape fragmentation characterized by forest patches interspersed with water bodies and channels may hinder moderate spatial resolution (MSR) images, provided with a pixel size of >4 m (such as Landsat or Sentinel-2 images) when mapping mangrove areas with accuracy and robustness. Small-scale changes might not get captured using MSR images until the fine-scale changes accumulate and result in major changes; at this point, it might be too late to mitigate.

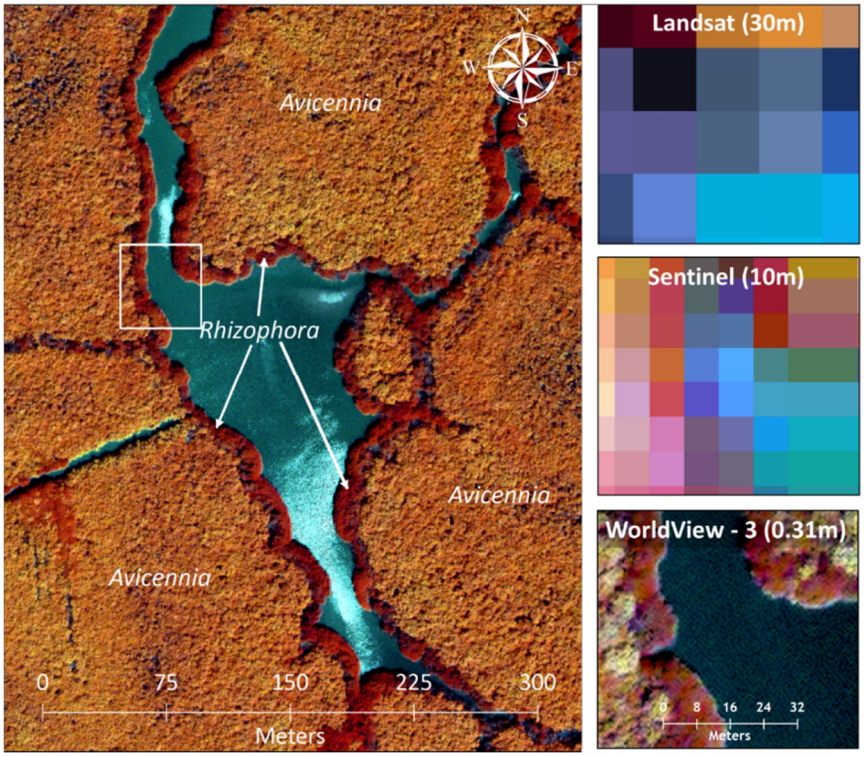

Figure 1. Importance of spatial resolution for mapping changes in mangrove cover. Mangrove subsets from MSR images from Landsat-8 (15 March 2019) and Sentinel-2 (31 May 2019), along with very high spatial resolution image Worldview-3 (28 January 2019).

For the better analysis of fine-scale changes and the implementation of rehabilitation or mitigation measures, the periodic monitoring of mangrove ecosystems using very high spatial resolution images (VHSR) satellite images delivered with a pixel size of finer than 4 m is necessary. Efforts to map mangrove habitats and analyze spatiotemporal changes using VHSR (Quickbird, GeoEye, Worldview) images are rare, but, when achieved,

valuable information about mangrove status has been obtained [18,20–25]. First, VHSR remote sensing supports the setting up of field experiments. Second, when combined with field surveys, VHSR remote sensing images are able to provide the fine-scale mapping of species distribution or biomass dynamics through the development of quantitative and robust remote sensing methods based on spectral and textural image characteristics [26,27]. Third, time series of high resolution images facilitate the accurate diagnoses of changes in mangrove habitats and allow for the questioning of the reasons for local demise or the establishment of mangroves [18,28,29].

In India, efforts to monitor spatiotemporal changes in mangrove habitats using VHSR images have been even less frequent [30,31]; mangrove rehabilitation measures have been generally assessed as successful solely from the monitoring of the surface, which have been estimated using moderate resolution images such as Landsat or IRS LISS-III [32,33]. The relevance of the plantation techniques, hastily referred to restoration practices, remains insufficiently questioned though multiple studies drawing attention towards the limitations of this approach [18,34], especially when the post-planting in situ monitoring of planted mangrove attributes is not carried out. This is the case of the fishbone plantation, a typical approach that has been in practice since the 1980s in India to (re)introduce mangrove on degraded lands [32]. This plantation method diverts water from existing creeks and channels through the construction of new channels, thus converting the barren land into an area that tides are expected to reach more easily and frequently, with expected impacts on the growth and survival of planted mangrove seedlings.

Here, we demonstrate the potential of VHSR remote sensing to study the Pichavaram mangrove region located in Southeast India based on the use of a time series of five VHSR satellite images acquired over a period of 16 years (2003–2019). This mangrove region is part of a major restoration program of wetlands of the east coast of India initiated in the 1990s by national and local authorities [32]. So far, changes in Pichavaram mangroves have been analyzed with moderate resolution images such as Landsat and IRS LISS-III [32,33]. As few ancillary data are available for scientific analysis, the current status of this mangrove area must be questioned. We therefore attempted to map mangrove habitats through an analysis of changes in the mangrove extent with the aim to identify and understand the environmental and anthropogenic driving forces, a number of them being exogenous to the mangrove area itself. A second objective was to assess the performance of the mangrove rehabilitation efforts that have been undertaken by the state forest department. In addition, as we identified a mangrove dieback event in Pichavaram that has resulted in massive tree mortality, we discuss the current status of the Pichavaram mangroves and provide recommendations to improve knowledge and monitoring of this fragile area.

2. Materials and Methods

2.1. Study Area

The Pichavaram mangrove is located almost 15 km northeast of Chidambaram in the Cuddalore District of Tamil Nadu. Based on the Köppen–Geiger system [35], climate in Pichavaram is tropical wet and dry (tropical savannah sub-type), characterized by hot and humid summers, with maximum temperatures reaching almost 42–45 degrees Celsius followed by mild and pleasant winters (average high temperatures of 25 degrees Celsius).

The mangrove region is bordered by the Vellar estuary in the north and the Kollidam estuary in the south (Figure 2). The total estuarine area is about 23 km^2, of which mangroves cover about 1100 ha [33,36]. The area is characterized by fertile alluvium deposits in the west that gradually change to fluviomarine deposits and beach sands towards the eastern area close to the Bay of Bengal. The mangroves receive most of their freshwater from the Kollidam River (rather than the Vellar River) due to the south–north elevation gradient. The region receives a majority of rainfall from the northeast monsoon (October–December), and to a much lesser extent from the southwest monsoon. From October to December, the freshwater input can generally increase considerably while the region remains dry [37], with salinity levels being very high (35–45 ppt) during the rest of the year [36].

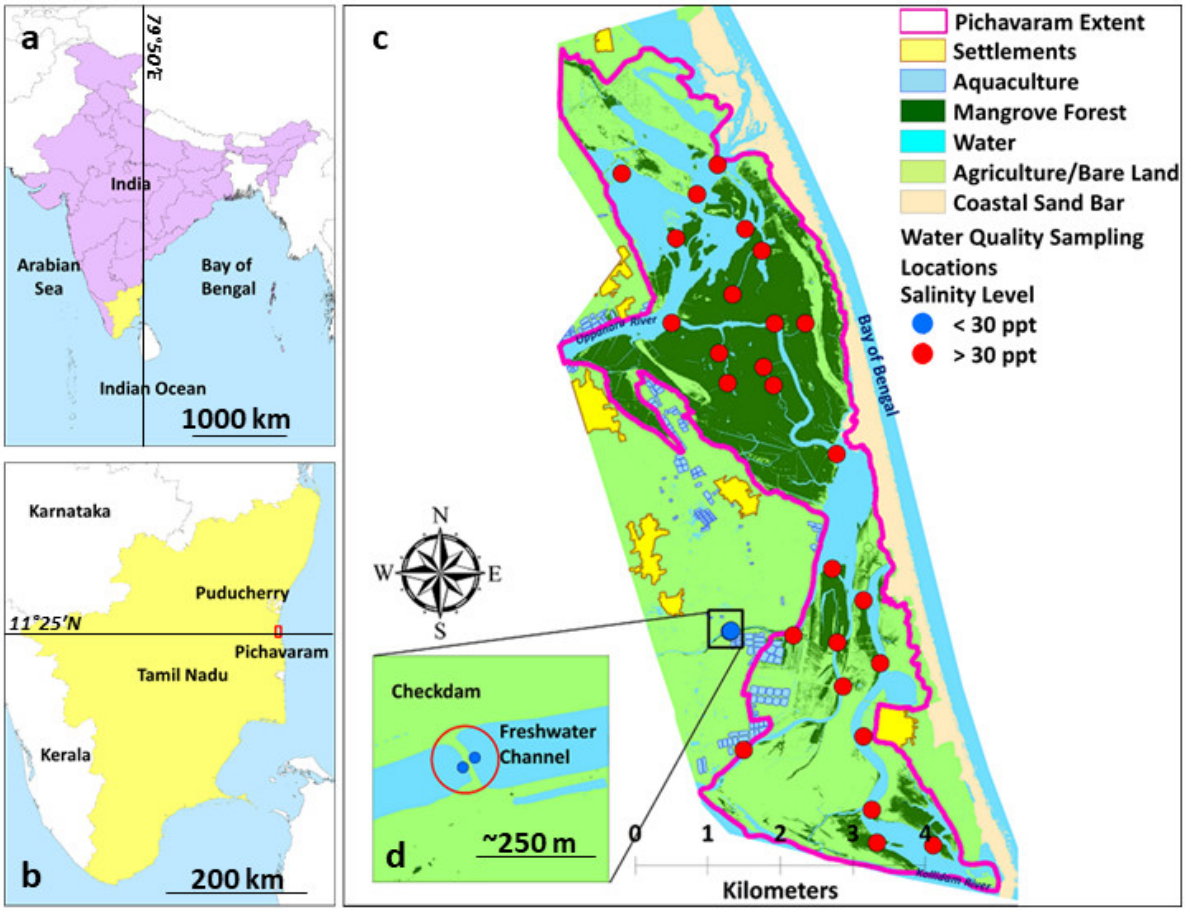

Figure 2. Location of the Pichavaram mangroves in Tamil Nadu, Southeast India (**a**,**b**). The mangrove area, along with the adjacent land-use and land-cover such as agriculture, aquaculture, check-dams on freshwater streams, and settlements, is illustrated (**c**). Locations of water quality samples are also shown along with the observed salinity levels (**d**).

The Pichavaram mangrove ecosystem is surrounded inland by fishermen hamlets, agriculture, and aquaculture ponds that have shown significant increases in numbers, especially in the last decade. The mangroves serve as lifeline for the surrounding coastal fishermen community. The fishery production harvested from the mangrove wetland has been reported to be almost 245 tons (prawns constituting almost 85% of the reported harvest) [36,38,39]. Almost 1000 fishermen seasonally fish in the mangrove; in addition, 800–900 cattle graze the mangrove wetland area, although the rates of cattle grazing have been reported to decline over the years [36]. The Pichavaram mangroves played a critical role in mitigating the devastating effects of the inundation resulting from the Indian Ocean Tsunami of 2004 on the hamlets that were guarded by the mangroves on the seaward side [31].

Today, the habitat is mainly dominated by *Avicennia marina* in the interior parts, while *Rhizophora apiculata* and *Rhizhophora mucronata* form the periphery of mangrove patches. Apart from *Avicennia* and *Rhizophora*, a few other mangrove plants have been intermittently observed in the ecosystem, such as *Bruguiera cylindrica*, *Excoecaria agallocha*, *Ceriops decandra*, *Avicennia officinalis*, *Aegiceras corniculatum*, *Rhizophora annamalayana*, *Acanthus ilicifolius*, and *Lumnitzera racemosa*, with some rare observations of *Xylocarpus granatum* and *Sonneratia apetala* [39]. No detailed data on mangrove forest structure are available. Based on personal visual inspection, *Rhizophora* formations along the river banks can reach heights of up to 6–7 m, while old and probably non-planted *Avicennia marina* (>20 years) may reach heights of 10–12 m. Tree height in plantations, where mangroves are mostly shrubby in nature, seems to be lower (<3 m). The state forest department has been implementing fishbone plots in Pichavaram since the 1990s in an

attempt to (re)introduce mangroves in the area, even on barren land (Figure 3). It is worth noting that, to our knowledge, the biogeochemistry, topography, and elevation of barren land are not documented prior or even after planting.

Table 1. Specifications and dates of acquisition of the VHSR images used in this study. The angles θs and θv denote the sun zenith and viewing zenith angles, respectively, while $\phi s–v$ is the relative sun-viewing azimuth angle. The tide levels during the time of acquisition, obtained from NOAA Tides and Currents (http://tidesandcurrents.noaa.gov, accessed on 12 November 2021) are also indicated. P = panchromatic; MS = multi-spectral.

Satellite and Format	Acquisition Date	Pixel Size (m)	θs (°)	θv (°)	$\phi s–v$ (°)	Tide Level (cm)
QBD [P, 4 MS]	4 May 2003	[0.6, 2.4]	22.8	6.5	292.6	7
	5 January 2005		38.7	32.9	230.3	46
GEO [P, 4 MS]	22 March 2011	[0.4, 1.6]	26.1	19.6	262.3	0
	30 January 2016		38.8	26.3	86.1	20
WV3 [P, 8 MS]	28 January 2019	[0.4, 1.6]	34.5	19.2	169.2	44

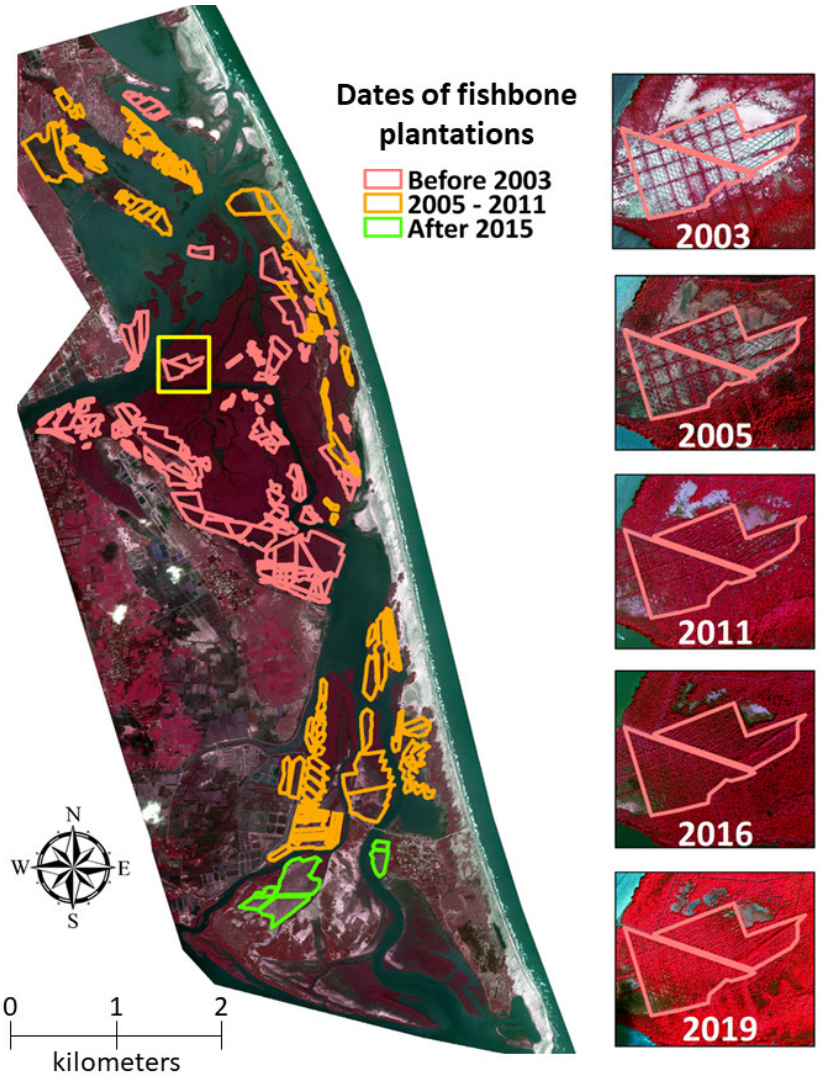

Figure 3. Pichavaram mangroves in Tamil Nadu along with the locations of the fishbone plots (**left**). Changes in the mangrove cover inside a 400 × 400 m fishbone plot (yellow square) implemented before 2003 are illustrated on the **right** using the VHSR image dataset described in Table 1.

2.2. Data

2.2.1. VHSR Satellite Imagery

We searched for cloud-free VHSR satellite images covering the Pichavaram mangroves on the Maxar® web-catalog. We shortlisted five images and purchased them; these comprised Quickbird (QBD) images from the years 2003 and 2005 (acquired a few days after the Indian Ocean Tsunami that had heavily impacted the region on 26 December 2004), GeoEye-1 (GEO) images from 2011 and 2016, and a Worldview-3 (WV3) image from 2019 (Table 1). All the images were captured at low tides. Each image was delivered in the GeoTIFF format as a set of two files, one comprising the panchromatic band (P) and the second one containing a multichannel stack generated by combining either four or eight multispectral (MS) bands, depending on the sensor. Panchromatic and multispectral bands were provided with pixel sizes ranging from 0.4 to 0.6 m and from 1.2 to 2.4 m, respectively. We selected the GeoEye image of 30 January 2016 as a reference image for the geo-registration of all the other images to Universal Transverse Mercator (Zone 44N). We estimated the spatial registration accuracy as 1–2 m for the satellite images.

The pixel intensity (or digital number) of satellite images was transformed into a TOA reflectance value, without correction for atmospheric effects, as follows:

$$\rho = \frac{\pi \cdot L_\lambda \cdot D^2}{E_{sun} \cdot cos\theta_s} \quad (1)$$

where ρ is the pixel reflectance, L_λ is the radiance obtained using sensor-specific equations provided in the image metadata files, D is the Sun–Earth distance (expressed in astronomical units), E_{sun} is the corresponding mean solar exo-atmospheric spectral irradiance ($mW.cm^{-2}.\mu m^{-1}$), and θ_s is the solar zenith angle [40]. In addition to the five raw VHSR multispectral images, we used RGB composites provided by the Google Earth platform at different dates between 2003 and 2019.

2.2.2. In Situ Water Quality

We conducted two field visits in the study area during the pre-monsoon season of 2019–2020 to measure in situ surface water salinity levels across a number of locations in the mangrove area (Figure 2) using the HI-98192 professional waterproof salinity meter. The instrument was calibrated prior to the field visits using an EC calibration solution. No field visits were possible during the post-monsoon season and the monsoon season of 2020–2021 due to travel restrictions imposed in response to the COVID-19 pandemic.

2.2.3. Meteorological Observations

We obtained monthly rainfall (0.25-degree grid) and air temperature (1-degree grid) data for the 1901–2019 and 1951–2019 periods, respectively, using meteorological observations from the Indian Meteorological Department (IMD) (https://mausam.imd.gov.in/ accessed on 12 November 2021) for the Cuddalore district in Tamil Nadu. From these long-term records, we investigated possible anomalies in precipitation and temperature regimes during our study period of 2001–2019 through a comparison of short-term and long-term linear trends.

2.3. Methods

Our main objective was to distinguish mangrove areas from non-mangrove areas to capture changes in the mangrove habitat. For this, we developed our analysis through a supervised classification process based on all panchromatic and multispectral bands available for each image, as described below. We did not use any vegetation indices.

2.3.1. Supervised Classification

Supervised classification was performed on each of the VHSR image using the nearest neighbor algorithm (see [41] for a review of image classification methods) in ERDAS Imag-

ine 2016 (Hexagon Geospatial; https://www.hexagongeospatial.com/products/power-portfolio/erdas-imagine accessed on 31 March 2022).

Due to lack of geo-registered in situ data on vegetation for the whole study period, species-level classification was avoided, while a generic land-cover level classification was conducted. From a visual inspection of VHSR images consolidated by our ground experience, training and validation polygons of an area ranging from 0.1 to 4 ha were delineated for three predominant land-covers, i.e., mangrove, water, and other non-mangrove areas (e.g., barren sandy and dry areas, sandy vegetation, aquaculture ponds, areas, roads, and buildings) in each image, mostly independently of each other. User's and producer's accuracy values were generated along with the kappa statistic, as well as overall accuracy. New training and validation polygons for each of the three land-covers were created and added to the classification process for each image until the maximum variability of spectral responses for each class was captured and the accuracy levels reached stable values. This was achieved through a few iterations for each image.

2.3.2. Land-Cover Change Detection

Comparisons were performed to detect changes in the whole Pichavaram region with respect to the initial land-cover of 2003 (such as comparisons between 2003 and 2005, 2003 and 2011, 2003 and 2016, and 2003 and 2019), as well progressive changes in land-cover since 2003 (comparisons between 2003 and 2005, 2005 and 2011, 2011 and 2016, and 2016 and 2019). The change classes generated through these comparisons comprised unchanged mangrove, water, and non-mangrove classes and the following changes (initial land-cover to subsequent land-cover): 'mangrove to non-mangrove', 'mangrove to water', 'water to mangrove', 'water to non-mangrove', 'non-mangrove to mangrove', and 'non-mangrove to water'. Progressive and cumulative mangrove gains and losses were derived since the beginning of the study period (2003). The analysis of the 'mangrove to water' or 'water to mangrove' classified areas along the 15 km of Pichavaram shoreline was expected to provide a fine-scale diagnosis of the eventual impact of coastal erosion or seaward mangrove progradation.

It was also crucial to document the changes within the non-mangrove areas in proximity to Pichavaram in order to highlight any natural or anthropogenic features or phenomena that might threaten the mangrove ecosystem health and resilience. For that, we visually inspected the changes within the Pichavaram adjoining areas using the raw VHSR scenes, along with images available through Google Earth at different dates.

2.3.3. Mangrove Cover Change in Fishbone Plantations

We wanted to analyze the success and/or failure rates in the fishbone plots implemented just prior to the Quickbird image acquisition of 2003 (Figure 3). For this, we visually delineated fishbone units on all VHSR images; plots were segregated based on the time of their implementation (i.e., plots laid prior to 2003, between 2005 and 2011, between 2011 and 2016, and between 2016 and 2019). Some fishbone plantation units were implemented close/adjacent to one another: if it was during the same timeframe, we gathered them into a singular unit assuming that the geographical and environmental conditions were likely to be identical.

For further analysis, we only retained the fishbone plots that were laid prior to 2003 and between 2005 and 2011, as only two areas with fishbone plots were observed between 2011 and 2016 (see "after 2016" in Figure 3) and the plots implemented after 2016 were captured only in the VHSR acquired in 2019. Based on the observed rates of growth, we classified the performance of fishbone units into three categories, i.e., 'high growth', 'moderate growth', and 'low growth' plots.

2.3.4. Delineation of Dieback Areas

In 2019, during a field experiment, we noticed tree mortality in fringing *Rhizophora* trees across a certain mangrove area of Pichavaram. We visually inspected all VHSR images

available from 2016 to 2019, including satellite images provided in Google Earth to estimate when dieback came up and how many hectares of mangroves were affected. This objective could not be achieved using MSR satellite images.

3. Results

3.1. Supervised Classification

The supervised classification of the VHSR images yielded a very high level of accuracy (Table 2). For most of the images, an overall mapping accuracy of >90% was achieved with kappa values of >0.85. For 2005, though the mapping accuracy levels were observed to be relatively lower (85% and kappa = 0.77). Within the overall accuracy, the mangrove mapping accuracy was observed to be mostly >90% (both producer's and user's accuracy), apart from 2005 and 2019 when the user's accuracy reached 84.8% and 86.8%, respectively, which could still be considered reasonably high.

Table 2. Classification accuracies of individual land-cover classes for Pichavaram, as obtained from the supervised classification of the VHSR images (QBD = Quickbird; GEO = GeoEye-1; WV3 = Worldview-3).

Year	Class Names	Producer's Accuracy	User's Accuracy	Kappa
2003 (QBD)	Mangrove	96.2%	93.8%	0.91
	Water	90.8%	98.8%	0.98
	Non-Mangrove	97.3%	91.2%	0.87
		Total Accuracy = 95%		*Kappa = 0.92*
2005 (QBD)	Mangrove	84.8%	97.5%	0.96
	Water	88.9%	70.0%	0.59
	Non-Mangrove	82.4%	87.5%	0.81
		Total Accuracy = 85%		*Kappa = 0.77*
2011 (GEO)	Mangrove	94.1%	100.0%	1
	Water	100.00%	97.5%	0.96
	Non-Mangrove	97.4%	93.8%	0.91
		Total Accuracy = 97%		*Kappa = 0.96*
2016 (GEO)	Mangrove	93.0%	100.0%	1
	Water	100.0%	98.8%	0.98
	Non-Mangrove	98.6%	92.5%	0.89
		Total Accuracy = 97%		*Kappa = 0.96*
2019 (WV3)	Mangrove	86.8%	98.8%	0.98
	Water	97.1%	82.5%	0.76
	Non-Mangrove	90.1%	91.3%	0.87
		Total Accuracy = 91%		*Kappa = 0.86*

The confidence attached to the temporal analysis of VHSR images was judged sufficient to map (Figure 4) and document spatiotemporal changes at fine scales of the main land-covers within the mangrove area itself and its surroundings.

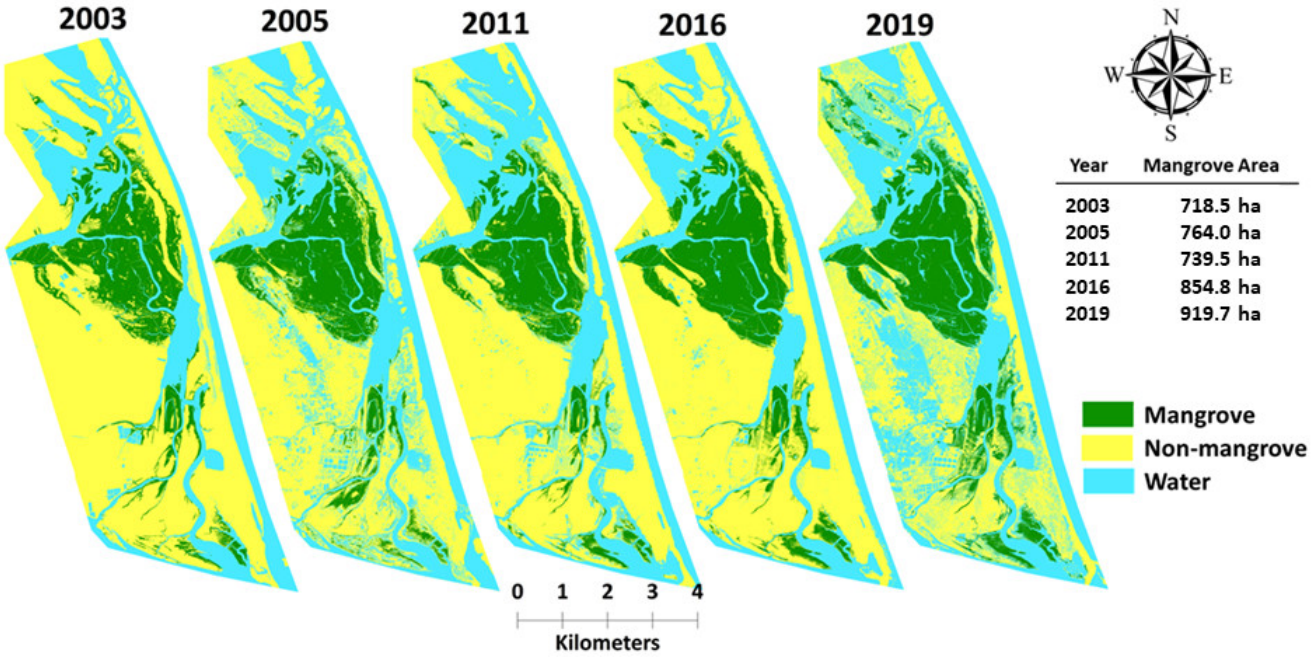

Figure 4. Land-cover maps produced from VHSR images (Quickbird for 2003 and 2005, GeoEye-1 for 2011 and 2016, and Worldview-3 for 2019) after supervised classification and visual adjustment; mangrove cover (in hectares) for individual years are mentioned.

Between 2003 and 2019, the overall mangrove cover of Pichavaram expanded by about 2 km^2, from 718.5 ha to 919.7 ha, (Figure 5a). The area of natural mangroves increased by 62 ha from 600 to 662 ha while the area of mangroves planted in fishbone plots expanded by about 139 ha from 118.5 to 257.7 ha.

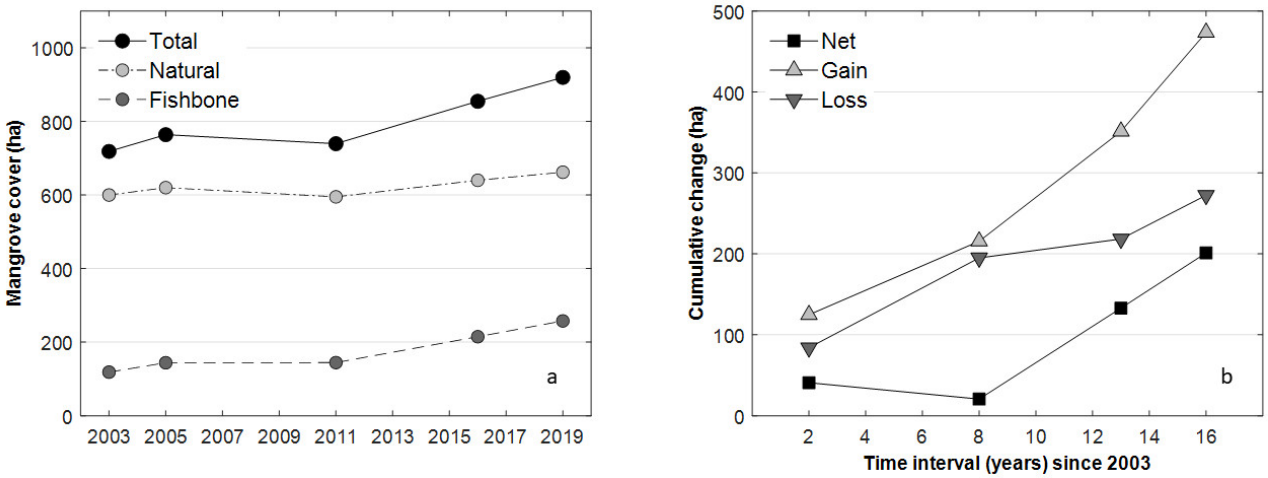

Figure 5. Change in cover among total, natural, and artificial mangrove area (**a**). Cumulative gross gain, gross loss, and net gain of mangrove cover at different time intervals since 2003 (**b**).

3.2. Change Detection and Analysis

The gain and loss in mangrove habitat have been gradual, with mangrove gross gains of 17.4% (124.8 ha), 30.0% (215.6 ha), 49.3% (354.1 ha), and 65.9% (473.6 ha) and mangrove gross losses of 11.7% (84.0 ha), 27.1% (195.0 ha), 30.4% (218.4 ha), and 37.9% (272.4 ha) at 2, 8, 13, and 16 year intervals, respectively (Figure 5b). The mangrove gross loss was always lower than the mangrove gross gain, and a net gain of mangrove areas of 28.0% (201.2 ha) relative to the mangrove cover of 2003 was assessed.

Looking more closely at the different change classes, it appears that the gain in mangrove areas mostly resulted from the conversion of non-mangrove areas to mangrove areas (Figure 6).

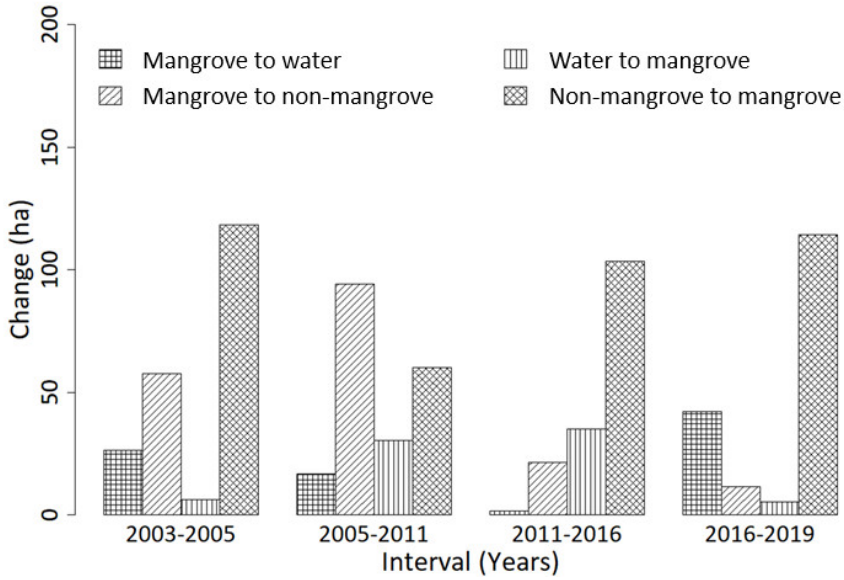

Figure 6. Progressive change in land-cover (in hectares) at image acquisition intervals.

Non-mangrove areas overall contributed to 396.4 ha of the mangrove growth between 2003 and 2019 with progressive increments of 118.5 ha (2003–2005), 60.3 ha (2005–2007), 103.4 ha (2011–2016), and 114.2 ha (2016–2019). Conversion from water to mangrove areas was also observed, albeit negligible, with an overall conversion between 2003 and 2019 of 2%. Conversely, we observed an overall combined loss of mangrove areas to non–mangrove or water areas with progressive losses of 84.1 ha (2003–2005), 81.9 ha (2003–2011), 61.8 ha (2003–2016), and 59.1 ha (2003–2019), this latter value corresponding to 8.2% of the mangrove area in 2003.

Looking at the change classes 'mangrove to water' and 'non-mangrove to water', we could detect changes in the shoreline (Figure 7).

Notably, the Quickbird image of early January 2005, 10 days after the Indian Ocean tsunami, revealed the disappearance of sandbars close to the mouth of the Uppanaru River (Figure 7a,b) and along the coastline near central Pichavaram (Figure 7f,g). However, in the subsequent images, no lingering effects of the apparent flood event were visible (Figure 7c–e,h–j) New sandbars visible in 2011–2019 images appeared near the mouth of the Kollidam River in the south (Figure 7k–o). Furthermore, a substantial extent of non–mangrove inland areas were apparently flooded, thus creating temporary water bodies in the 2005 image (waterlogging as an aftereffect of irrigation; discussed later) (Figure 7p–t) that were converted back to non-mangrove areas between 2005 and 2011 (waterlogging was not observed in 2011).

In addition, we observed a constant and progressive conversion of non-mangrove areas to water areas along the coast, indicating shoreline erosion, while new non-mangrove areas were being formed in the southern part of Pichavaram (particularly near the mouth of the Kollidam River) as a probable response of sediment deposition. These latter areas were not colonized by mangroves in 2019.

The construction of artificial channels within the mangrove area itself, as well as the construction of artificial pond-like structures (Figure 8a–e) or artificial barriers (Figure 8f–j) across upstream channels, could be observed along the periphery of the Pichavaram mangrove forests and further inland.

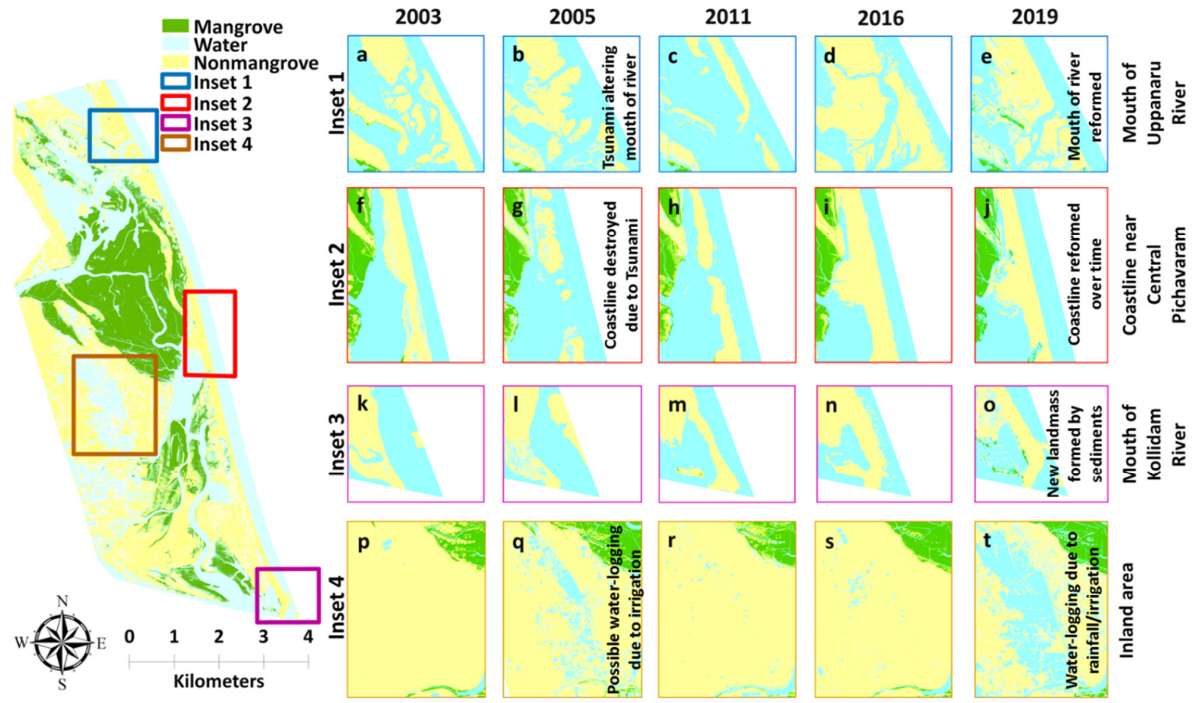

Figure 7. Changes, with a focus on the land (mangrove or non-mangrove) to water changes, in the land-cover of Pichavaram area and surrounding areas such as (**a**–**e**) the mouth of the Uppanaru River, (**f**–**j**) coastline near the central Pichavaram forest, (**k**–**o**) the mouth of the Kollidam River, and (**p**–**t**) inland area.

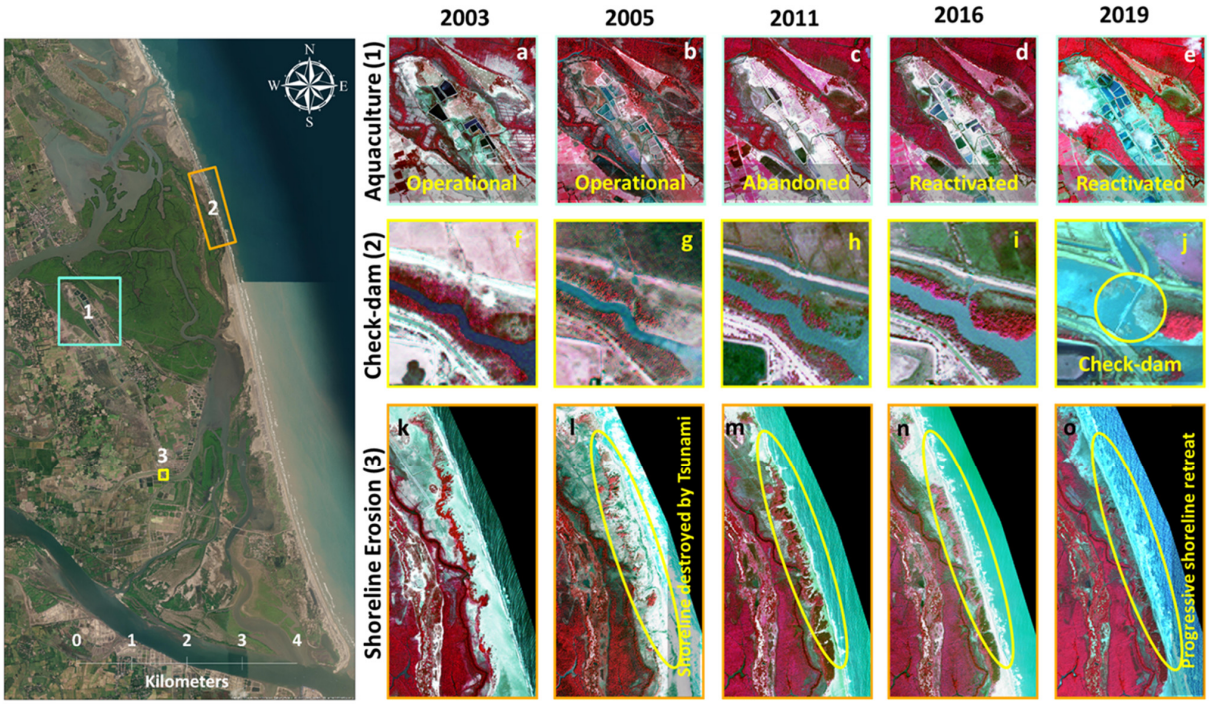

Figure 8. Changes observed in the land-cover of Pichavaram mangroves and the surrounding areas from the visual inspection of the VHRS images (image excerpts on the **right**) in combination with a 2016 color-composite image provided by Google Earth (**left**). Aquaculture expansion in the vicinity of the mangrove forest (**a**–**e**), check-dam construction in freshwater channel to Pichavaram (**f**–**j**), and progressive shoreline erosion (**k**–**o**) can be easily identified and monitored.

3.2.1. Change in Mangrove Cover within Fishbone Plantations

Overall, we observed a gradual increase in the mangrove cover within the fishbone areas (Figure 9a). The annual expansion rate of the mangroves within the fishbone plots implemented prior to or in 2003 was about 1.7% but could reach 4% for a number of plots where mangrove cover was between 20 and 40% in 2003. However, a number of plots showed minor loss in mangrove cover, and a single fishbone plot, located close to the mouth of the Uppanaru River, did not show an expansion of its mangrove cover during the entire study period (Figure 9a, bottom evolution profile).

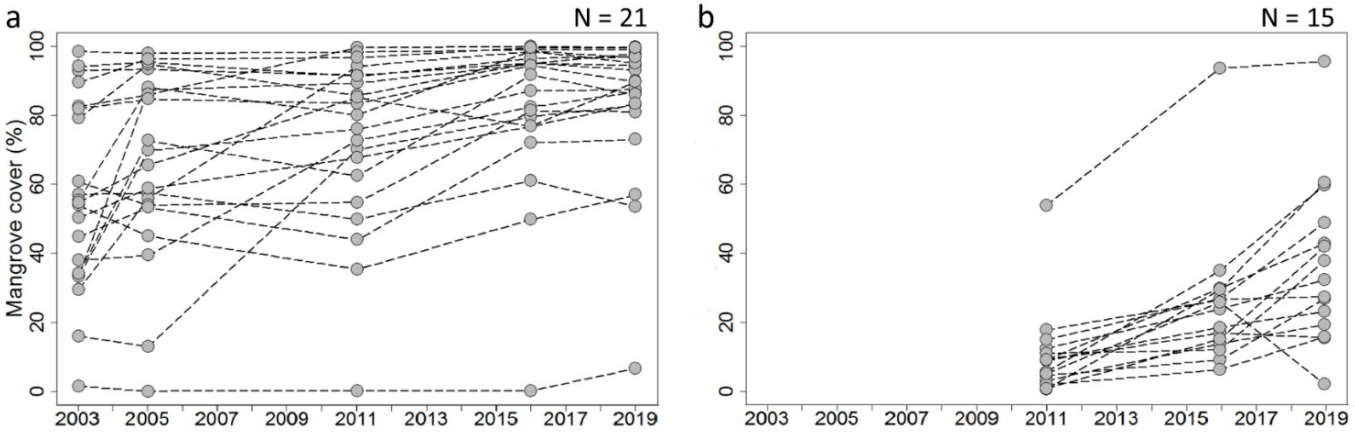

Figure 9. Changes in the mangrove cover (% relative to fishbone area) within individual fishbone plots implemented prior to or in (**a**) 2003 and (**b**) between 2005 and 2011.

A similar trend (Figure 9b) was observed for the fishbone plots implemented between 2005 and 2011, with most of the plots reaching between 20 and 60% of mangrove cover by 2019. The annual mangrove expansion rates observed within plots ranged from 0.4% to 3.5%, with an average growth rate of 1.7%—values very similar to those observed for the plots implemented prior to or in 2003.

3.2.2. Dieback in Natural Mangroves

Mangrove dieback in the central west Pichavaram area (Figure 10a), first reported by the forest department in late 2008, was confirmed by our in situ observations in 2019 (Figure 10d).

We observed that the phenomenon was affecting only a number of river-fringing *Rhizophora mucronata* trees along about 1.5 km of river banks. From a closer visual inspection of the GeoEye image of January 2016 with support from the Google Earth VHSR satellite images of April and November 2017, we estimated that tree defoliation started in 2017 (between April and November) along the river banks of a 2.5 ha water basin located 700 m eastward of active aquaculture ponds, impacting a mangrove area of 0.8 ha. The majority of the dieback was noticed along three interior channels, two southward and one northward from a branch of the Uppanaru river, and mortality was observed along both sides of the channels. In total, the phenomenon was observed along 2 km of fringe mangrove area along several channels (Figure 11a).

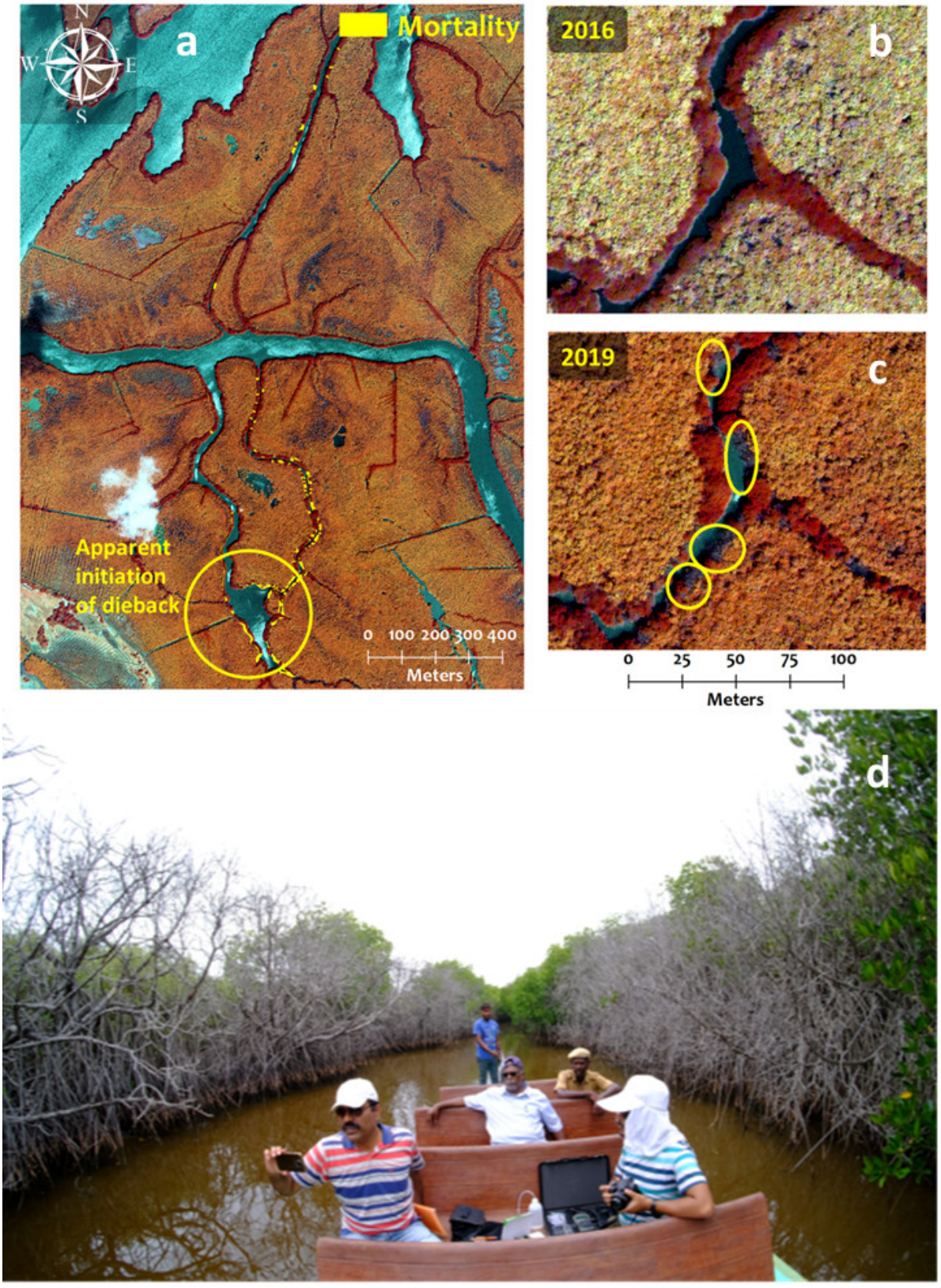

Figure 10. *Rhizophora* dieback spots in Pichavaram highlighted from the 2019 Worldview-3 image (**a**). Inset images show areas with presence of *Rhizophora* in 2016 (**b**) and subsequently dieback in 2019 (**c**), as confirmed by in situ observations (**d**).

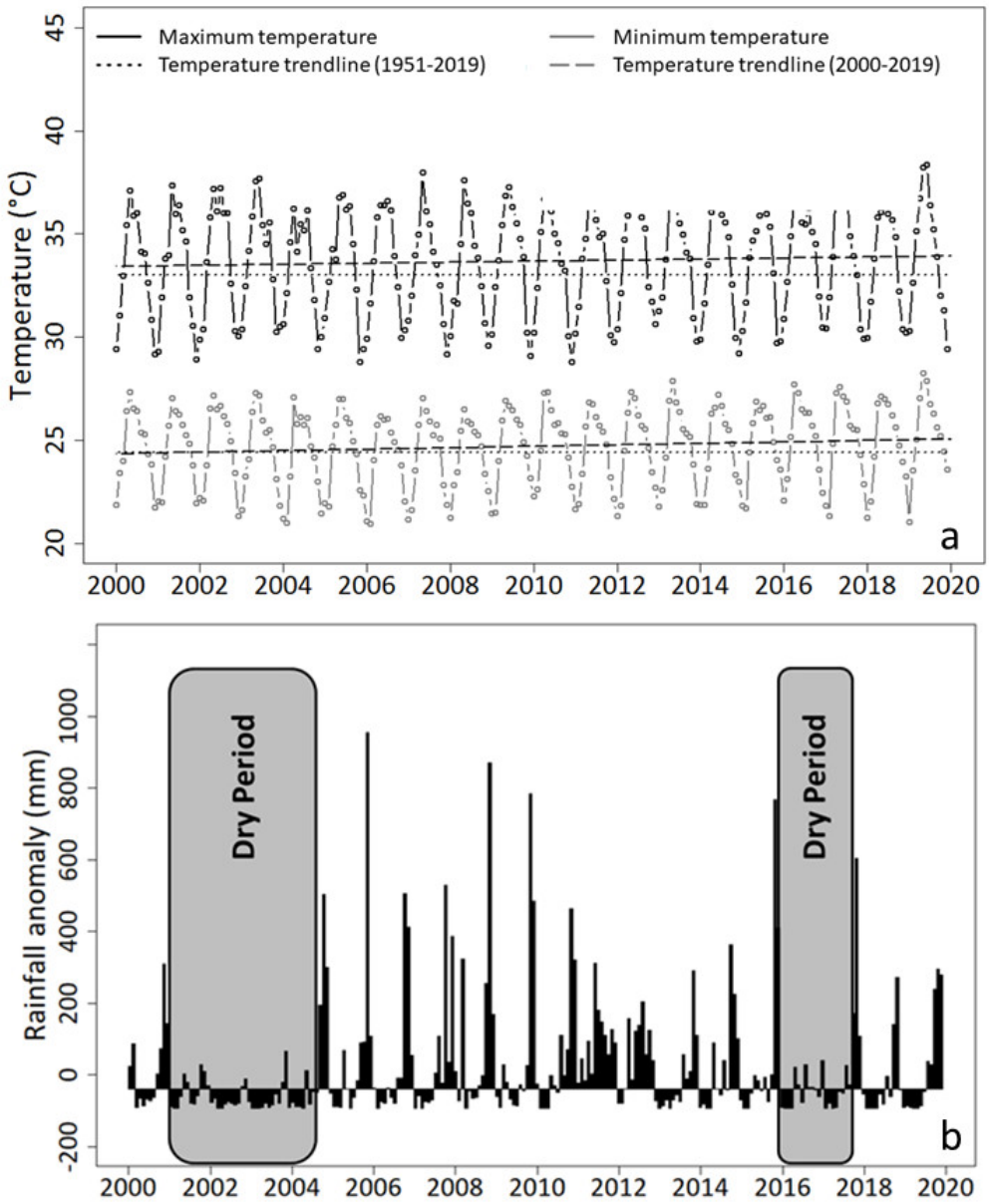

Figure 11. Air temperature for Cuddalore, near Pichavaram. Monthly maximum and minimum temperatures are provided for the time period of 2000−2019. Linear trends for both the 1951−2019 and 2000−2019 time periods are also indicated (**a**). Median rainfall anomalies for Pichavaram from 2000 to 2019 (encompassing the study period) are presented. Abnormal dry periods from 2001 to 2005 and from 2016 to 2017 are highlighted (**b**).

3.2.3. Additional Diagnostics Based on Meteorological Observations and Water Salinity

Overall, maximum air temperature ranged between 27.3 and 38.3 degrees Celsius for the time period of 1951–2019 and between 29.7 and 38.2 degrees Celsius for the time period of 2000–2019 (Figure 11a). Monthly minimum and maximum temperatures increased by an average of 1.37 and 1.77 degrees Celsius, respectively, over the 1951–2019 period in the Pichavaram region. Both the minimum and maximum air temperature trends showed gradual increases over the two time periods (with a steeper increase in minimum temperatures over the last 20 years than over the long-term period), as measured by the upward slopes of the trend lines that were 0.0356 and 0.02573, respectively.

Regarding median monthly rainfall data (Figure 11b), the analysis showed two exceptionally dry periods between 2001 and 2005 and between 2016 and 2017. A rainfall surplus was observed throughout 2011.

Salinity levels (data not shown) recorded from the water samples collected during our field visits (see location of samples in Figure 2) ranged from 30 parts per thousand (ppt) to 38 ppt, which is comparable to sea-level salinity. Low salinity levels (<1 ppt; comparable to freshwater salinity level) were observed only in two locations, close to each other, in the vicinity of a check-dam that was recently constructed upstream of the mangrove area (Figure 2d).

4. Discussion

4.1. Mangrove Cover Estimates Using Very High Spatial versus Moderate Spatial Resolution Images

The VHSR-based mangrove cover estimates (from 718 ha in 2003 to 919 ha in 2019) were consistently lower than the Landsat-derived mangrove cover estimates (from 800 ha to 1078 ha) for the same study area (Figure 12).

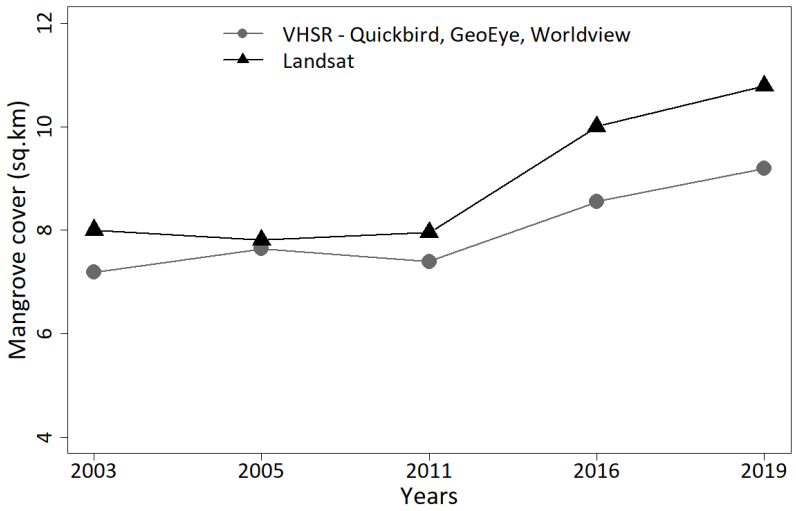

Figure 12. Comparison of mangrove cover as estimated by VHSR images (Quickbird, GeoEye, and Worldview) and Landsat.

The Landsat-image-based mangrove cover was in much greater agreement with the estimates of mangrove cover provided in earlier studies [30,36] that used moderate resolution sensors for mapping mangrove vegetation in Pichavaram. This difference may be attributed to the more accurate level of detail captured by VHSR images compared to that of moderate resolution images. The geomorphology of mangroves is often characterized by fragmentation, with patches of vegetation interlaced by water channels and small open water bodies. Unlike VHSR images, moderate resolution sensors often classify otherwise mixed pixels as vegetation, resulting in overestimates of mangrove vegetation (Figure 1). This study emphasizes the need to map complex and fragmented habitats such as mangroves using VHSR images, especially while studying very localized mangrove habitats such as Pichavaram. The methodology used in this study may not be novel and the results demonstrating the robustness of VHSR may not be unexpected. However, in the case of the Pichavaram mangrove forest, an analysis of time series of VHSR images acquired over 16 years proved to be particularly interesting to highlight the range of fine-scale positive or negative evolution trends of the mangrove habitats through an up-to-date diagnosis of the mangrove situation, where a lack of in situ data has been an impediment.

4.2. Monitoring Spatio-Temporal Changes in Mangroves Using Time Series of VHSR Images

The majority of the VHSR images were classified with a >90% accuracy. From the confusion matrix, it is clear that the mapping accuracies of the individual land-covers were affected by the presence of water (particularly in the Quickbird image from 2005), which may have been either residual moisture or actual sea-water logged in both open-mangrove and non-mangrove areas. This is not entirely unexpected due to the contrasting spectral responses of aquatic and non-aquatic surfaces, which hinders the performance of both supervised and unsupervised methods of classification. Satellite images of coastal regions and ecosystems in particular are often influenced by tidal water fluctuations. Therefore, image acquisitions at low tide may guarantee desired levels of accuracy. As suggested by the high-level accuracy reached for the classification of the GeoEye image of 2011, a year with rainfall surplus, steeper viewing zenith angles along with adequate sun-viewing azimuth angles may help mangrove areas to be discriminated from water areas. Sun-frontward angle configurations must be particularly avoided to limit sun backscattering from water areas, as observed and explained in [18].

Further, this analysis highlights the robustness of the VHSR images in capturing details of the changes that have occurred in the mangrove ecosystem including progressive gain and loss of mangrove habitat since 2003. The ecosystem itself is very dynamic, with constant changes taking place at a very fine spatial scale. As evident from Figure 13, changes that were captured by the VHSR images in this study would otherwise be difficult to observe and analyze using moderate or coarse resolution images.

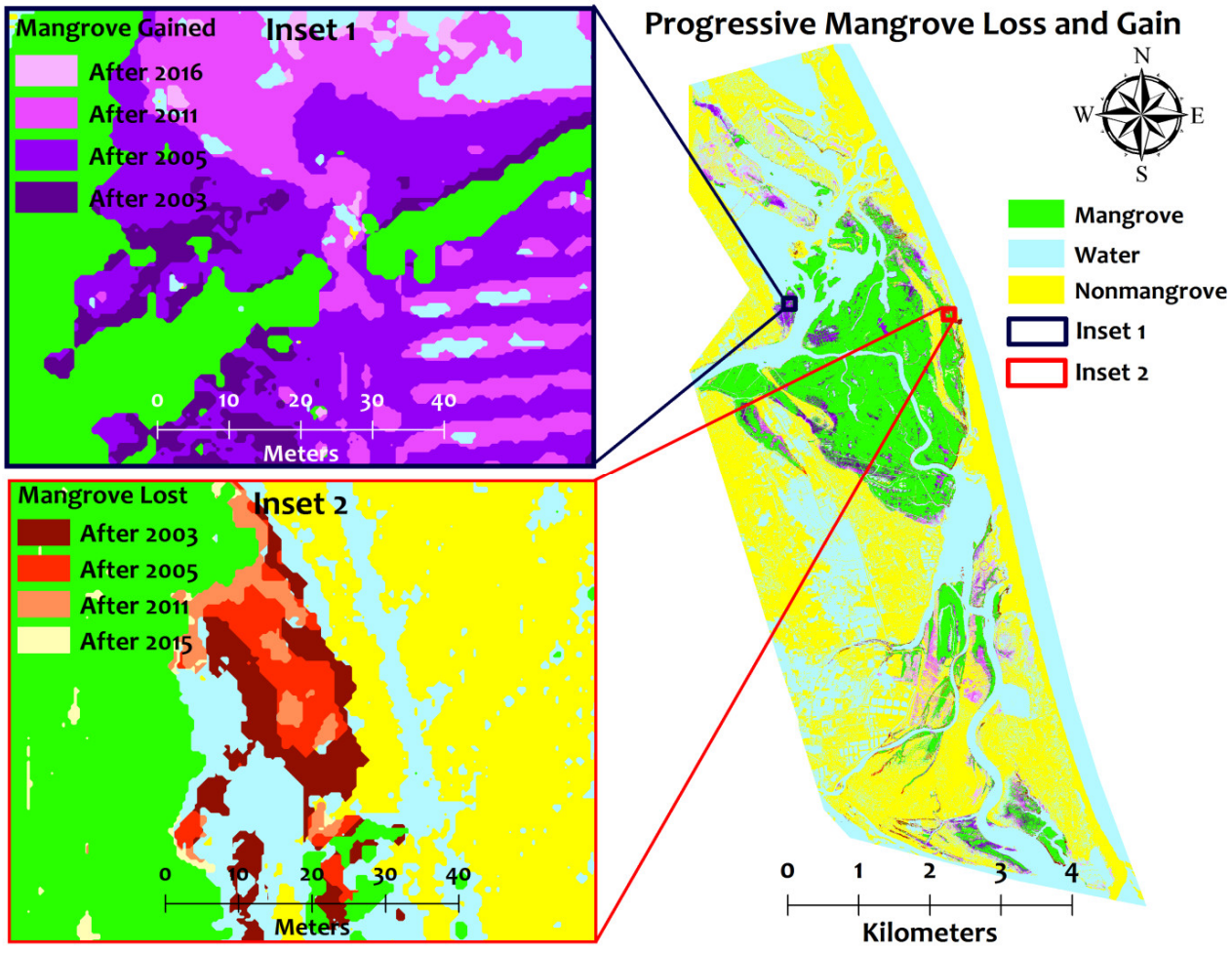

Figure 13. Mangrove gains and losses as captured by VHSR images at different time intervals in Pichavaram.

The visual inspection of VHSR satellite images provided by Google Earth is often helpful and complementary to the analysis of any multispectral images. The performance of the supervised classification of mangroves areas based on Google Earth VHSR false-color composites deserves further analysis.

Despite the robustness of the VHSR images in capturing spatial details, the lack of in situ observations has been a great impediment towards mapping the Pichavaram mangroves at the species level. Although the existing literature provides some basic information about the existing mangrove vegetation community [42,43], it is very difficult to match this information with the VHSR image data without any accurate spatial and ground reference of species identification and distribution. From our in situ observations and literature records, we can safely assert the domination of *Rhizophora* sp. along the river edges and *Avicennia marina* in the interior mangroves. However, mapping and identifying the co-existing species from multispectral VHSR satellite images remains difficult without accurate in situ observations. Even from the structural point of view, mapping species distribution in Pichavaram remains complicated. The forest canopy in the interior mangroves is formed by tree crowns of few square meters, either densely distributed with uniform tree height or sparsely located in the case of fishbone plantations. In such a scenario, even the use of sophisticated textural or combined spectral–textural approaches [26,29] applied on VHSR images for mapping and monitoring species has its limitations [44]. This aspect could be addressed in the future using a combination of active sensors, such as LiDAR, along with extensive in situ field observations of species location and canopy structure and size. Utilizing LiDAR may also facilitate understanding coastal geomorphology, more specifically erosion and the accumulation of sediments, shoreline retreat, and sea-level rise, factors which will determine the current and future sustainability management of the Pichavaram mangroves.

4.3. Preliminary Diagnosis for the Pichavaram Mangroves

4.3.1. Land-Cover Conversion to Mangrove Area

We observed a considerable extent of non-mangrove areas being converted to mangrove from our change analysis over a period of seventeen years. This conversion was mostly the result of the efforts undertaken by the state forest department to (re)introduce mangroves in Pichavaram through the implementation of fishbone plantations.

4.3.2. Mangrove Cover Fluctuations

However, in addition to the increment in mangrove cover, losses in mangrove areas were also observed, albeit to a lesser extent. Most of the losses in mangrove areas were observed from 2003 to 2005 and then from 2016 to 2019. The loss in mangroves from 2003 to 2005 may be attributed to the effects of the Indian Ocean Tsunami in December 2004. The mangroves also witnessed the landfall of Cyclone Thane in late 2011. However, they may have recovered in the subsequent five-year gap, as no mangrove decline was observed between the 2011 and 2016 images. Since no VHSR images were captured immediately after the landfall of the cyclone, the estimation of any mangrove damages whatsoever due to the landfall has not been possible. The loss in mangrove between 2016 and 2019 may be partly attributed to the mangrove dieback that was reported in the later part of 2017, which resulted almost 1 ha of *Rhizophora* being lost by 2019.

We did observe mangrove losses in years between 2005 and 2016 in our analysis; however, we did not have any in situ observations or studies on mangrove losses in Pichavaram at such a fine spatial scale that allowed us ascertain the causal factors behind the observed losses. Therefore, we can probably attribute the losses to possible localized environmental disturbances.

4.3.3. Effects of Tsunami and Shoreline Erosion

The destruction of the sandbars at the mouth of the Uppanaru River and the coastline in central Pichavaram can be clearly attributed to the devastating effect of the Indian Ocean

Tsunami of 2004 that was captured by the Quickbird image acquired just 10 days after the incident. The visual inspection of the 2005 image showed the effect of the tsunami, mostly along the coastal areas and to a lesser extent on the inland areas (Figures 4 and 7a–e). These sandbars were reformed in time, most likely as a result of the deposition of both riverine and marine sediments. In addition, we also observed progressive shoreline erosion along the eastern boundary of the Pichavaram mangroves and sediment accumulation leading to shoreline creation along the mouth of the Kollidam River, which borders the mangrove ecosystem in the south (Figure 7f–o) The progressive shoreline retreat might be disastrous to the mangroves of Pichavaram, as it might lead to sandy bars encroaching on mangrove habitat or the creation of a perennial hypersaline environment due to seawater inflow that may lead to salinity-induced stress, particularly among the emergent mangroves, both natural and artificially planted in fishbone plots. The Pichavaram mangroves are already facing significant long-term threats from climate-change-induced sea-level rises in the northern Indian Ocean coastline [45].

4.3.4. Agriculture, Aquaculture and Other Developmental Activities

We also observe inland non-mangrove areas being converted to water from 2003 to 2005; this temporary conversion could be attributed to effects of irrigation practices. In addition, a lot of inland non-mangrove areas were converted to water bodies from 2016 to 2019. On a closer visual inspection of the raw image, these areas were found to be mostly agriculture and dry aquaculture ponds that were water-logged, probably due to rainfall accumulation or irrigation practices, just before the acquisition of the Worldview image of 2019. In addition, we observed the progressive expansion of aquaculture ponds close to the mangrove boundary throughout the 16-year study period.

While some of the aquaculture ponds may have been abandoned over time (hence, we observed these ponds to be colonized with natural vegetation), the majority of them remained apparently active. These anthropogenic practices should be regularly monitored, and any possible evidences of effluent discharge from these systems into the mangrove ecosystem should be investigated. The legal prohibition of such activities should also be considered if such activities are found to affect the mangrove ecosystem. In terms of any possible effect of the aquaculture practices on the Pichavaram mangrove ecosystem, opinions have been ambiguous [46,47] (discussed in Section 4.3.6).

In addition, we observed the construction of recent check-dams across freshwater streams flowing into the Pichavaram mangrove forest. These dams were constructed with the intention of restricting saltwater intrusion into upstream agriculture, though, in the process, these structures have also impeded the flow of freshwater into the mangrove ecosystem, which otherwise is critical for mangrove ecosystem functioning. Therefore, a mechanism for regulating the flow of freshwater into the mangrove ecosystem should be implemented.

4.3.5. On the Mangrove Rehabilitation Efficiency

Most of the fishbone plots implemented in 2003 showed gradual improvements in mangrove cover, with a gain of about 1.3 km^2 between 2003 and 2019. The mangrove cover in the fishbone plots implemented between 2005 and 2011 had also improved and will hopefully achieve complete mangrove cover in due course if environmental conditions remain favorable.

The particular fishbone plot that showed negligible mangrove growth during the sixteen-year time period was very close to the mouth of the Uppanaru River, an area most likely directly impacted from the Indian Ocean Tsunami in 2004 that may have destroyed any mangrove saplings planted there. Any chance of a quicker recovery may have been hampered by the landfall of Cyclone Thane in late 2011. The fishbone plots that had not shown any significant improvement in mangrove cover need to be revisited and periodically monitored, and any possible reason for the reduced mangrove growth rate should be investigated.

This improvement in overall mangrove cover highlights the apparent success of the rehabilitation and conservation measures that have been implemented so far by the state Forest Department of Tamil Nadu. However, there has been no attempt to assess the efficiency of the restoration measures implemented in Pichavaram so far. This is the first study to provide a quantitative assessment of the efficiency of the restoration efforts at the finest possible scale, and it further emphasizes the importance of the periodic monitoring of the Pichavaram mangroves for the future assessment of the success/failure of the current/ongoing restoration efforts and their possible effects on the mangrove ecosystem. Whether the monoculture plantations by the Forest Department contribute to the long-term sustainability management of the Pichavaram mangroves or to reducing biodiversity leading to ecological complications in the future remains to be ascertained.

Therefore, we argue that the increase in mangrove cover cannot be the sole objective of future coastal management plans by the state forest department. The Pichavaram mangrove environment is already hypersaline, possibly owing to erratic rainfall-induced freshwater fluctuation and deficits along with rising minimum temperatures, resulting in more frequent hot and dry periods [45]. Further, the construction of check-dams upstream for preventing salt-water intrusion has also reduced the inflow of freshwater into the mangroves. Unless a policy for regulating freshwater inflow into the mangroves is implemented, such persistent hypersaline conditions may prove to be detrimental to newly planted mangrove saplings, resulting in reduced mangrove growth or even sapling mortality. Historically, hypersaline conditions have severely affected the existing plant diversity in Pichavaram, with extreme halophytic plants becoming dominant in the mangrove landscape, thus reducing the distribution of the less halophytic plant species [42,43,48]. Low plant diversity may be a precursor for ecosystem collapse, especially in an event of a widespread dieback or disease, from which mangroves may not recover from.

Furthermore, the sites for implementing restoration measures need to be carefully chosen, considering all the environmental factors that may affect mangrove growth and recovery and, ultimately, the success of the restoration effort. Care should also be taken in terms of choosing the right species for plantation [49] and restoring plant diversity along with vegetation cover to ensure proper ecosystem structure and functioning. Alternatively, just restoring the environmental conditions suitable for mangrove regrowth and survival may foster natural mangrove recovery [50].

4.3.6. Mangrove Dieback

Possible causes of mangrove dieback are plenty; studies have linked mangrove dieback to a multitude of factors, such as local herbivory [51], hurricane landfall [52], gale storm and wind gusts [53], iron toxicity [54], sea-level rise [55], drought [56], and even localized herbicide usage [57]. Therefore, it is difficult to ascertain the exact cause of the dieback observed in Pichavaram. A persistent hypersaline environment may be a reason; we have observed water salinity levels in Pichavaram comparable to sea level salinity in the dry season. However, salinity levels are usually lower in the wet season in this region, when the mangroves receive substantial freshwater from precipitation and river discharge. Earlier water quality studies in Pichavaram [37], along with careful observations of the site-specific meteorological data (i.e., temperature and rainfall) indicated severe fluctuations and progressive reductions in the level of freshwater coming into the mangrove ecosystem owing to erratic rainfall patterns and increasing temperatures, something that can be traced back to the first decade of the 21st century.

Again, we do not have any in situ observations of salinity from the wet season, as fieldwork was not possible due to the restriction of activities as a result of COVID-19-induced restriction measures. Additional in situ observations and estimations of water and soil bio-geochemistry are required to analyze whether there are any possible connections between salinity levels and/or freshwater discharge and mangrove mortality/dieback.

Further, as observed during the change analysis, human activities, especially aquaculture, have gradually increased in the vicinity of the Pichavaram mangrove ecosystem.

Although early observations had ruled out any negative effects of aquaculture practices on the mangrove ecosystem [46], current observations indicate the presence of shrimp farms and subsequent farming practices (sometimes illegal) responsible for the discharge of effluents and chemicals leading to fish and bird population declines, along with the introduction of invasive species in the ecosystem, all of which have caused damage to the ecosystem itself and the economy of the fishermen [47]. Therefore, a possibility of these chemical discharges into the adjacent mangrove ecosystem causing tree mortality cannot be ruled out. However, we need more evidence in the form of in situ bio-geochemical observations to substantiate this possibility.

4.4. Preliminary Recommendations for the Pichavaram Mangroves

We insist on the necessity of the continuous monitoring of the Pichavaram mangrove ecosystem to highlight the hotspots of mangrove degradation, as well as the subsequent prioritization of appropriate fine-scale restoration and conservation measures. For this purpose, the present analysis confirms the robustness of VHSR images in capturing details of the changes that have occurred in the mangrove ecosystem compared to previous studies conducted using coarser spatial resolution imagery [36]. Implementing a supervised classification of VHSR images remains quite intuitive because image interpretation matches the scale of human perception of mangrove attributes and environment features in the field. For the large-scale analysis of change in mangroves, the use of MSR images remains complementary.

However, as the tremendous potential of VHSR images in studying mangroves cannot compensate for the lack of in situ observations, initiatives to carry out regular in situ scientific forest inventories for describing forest structures and species distribution, along with abiotic parameters such as soil and water quality parameters (salinity and other biochemical properties), should be supported and encouraged by the local authorities to provide early warning in case of stress events [17], as experienced in Pichavaram [32,37].

The implementation of socio-ecological regulations for the integrated management and exploitation of mangrove resources is of prime urgency for the sustainability of both the mangrove forest and the livelihood of the fishermen community [38]. Indeed, progressive shoreline erosion, freshwater deficits, rising temperatures, and massive dieback are factors that are already threatening the mangroves of Pichavaram. Furthermore, any major environmental disturbance in the future such as a cyclone landfall or a tsunami could make the recovery of the mangroves very difficult, resulting in the unfortunate collapse of the mangrove ecosystem. This would, in turn, severely affect the livelihood of the surrounding coastal community (mostly fishermen), which is dependent on the sustenance and well-being of the mangrove ecosystem for their survival.

Finally, conservation decisions need to consider not only the environmental dynamics within the mangrove ecosystem but also the developments taking place outside of it [58]. The threat of developmental projects such as hydrocarbon exploration has already been perceived as a significant threat to the Pichavaram mangrove ecosystem [59]. Therefore, a holistic approach towards the conservation of coastal wetlands such as the Pichavaram mangroves is critical to the resilience of both the mangrove ecosystem and the livelihood of the local coastal community [60].

5. Conclusions

This study is the first known attempt of utilizing VHSR images for mapping and analyzing spatiotemporal changes in the Pichavaram mangroves. Our work also provides the first fine-scale in-depth assessment of the success of the fishbone plantations implemented by the forest department for restoring mangroves in Pichavaram. We also report widespread dieback and tree mortality among the fringe mangroves of Pichavaram, more specifically in *Rhizophora apiculata*. Our approach can be replicated to study and analyze similar mangrove ecosystems within coastal India and beyond, where the lack of ancillary data might be an impediment. Through the study of the Pichavaram mangrove region,

we illustrated how VHSR images can provide robust and crucial information on fragile mangrove regions in a simple manner, especially where there are an apparent lack of forest data and infrequent monitoring. This remains a prerequisite to diagnose ecosystem status, identify stressful conditions, and warn against rapid degradation.

Author Contributions: Conceptualization, S.G., C.P. and G.M.; Investigation, S.G., C.P. and G.M.; Writing—original draft preparation, S.G. and C.P.; Writing—review and editing, All authors; Image interpretation, All authors; Supervision, C.P.; Project administration, G.M., C.P. and R.M. All authors have read and agreed to the published version of the manuscript.

Funding: This research was funded by the Agence Nationale de la Recherche (ANR) via the Economic and Social Research Council, ESRC (UK) and EU–India Platform for Social Sciences and Humanities (EqUIP) program (ES/R010404/1) in the frame of the FISHERCOAST project (Coastal transformations and fishing community wellbeing—synthesized perspectives from India and Europe). The travel and research stay of C.H. and V.H. were supported by the Leibniz Centre for Tropical Marine Research (ZMT) from the Institute's core funding from the Federal Ministry of Education and Research and the State of Bremen.

Data Availability Statement: The data presented in this study are available upon request to the corresponding author.

Acknowledgments: The authors acknowledge K. Kathiresan, R. A. James, C. Lakshumanan, and T. Usha for kindly providing the independent validation data set of this project. The authors thank the Tamil Nadu Forest Department for allowing us to undertake this study.

Conflicts of Interest: The authors declare no conflict of interest.

References

1. Ellison, J.C. (Ed.) *Biogeomorphology of Mangroves*; Elsevier: Amsterdam, The Netherlands, 2019; pp. 687–715. [CrossRef]
2. Rovai, A.S.; Riul, P.; Twilley, R.R.; Castañeda-Moya, E.; Rivera-Monroy, V.H.; Williams, A.A.; Simard, M.; Cifuentes-Jara, M.; Lewis, R.R.; Crooks, S.; et al. Scaling mangrove aboveground biomass from site-level to continental-scale. *Glob. Ecol. Biogeogr.* **2016**, *25*, 286–298. [CrossRef]
3. Bunting, P.; Rosenqvist, A.; Hilarides, L.; Lucas, R.M.; Thomas, N. Global Mangrove Watch: Updated 2010 Mangrove Forest Extent (v2.5). *Remote Sens.* **2022**, *14*, 1034. [CrossRef]
4. Duke, N.C.; Meynecke, J.O.; Dittmann, S.; Ellison, A.M.; Anger, K.; Berger, U.; Cannicci, S.; Diele, K.; Ewel, K.C.; Field, C.D.; et al. A world without mangroves? *Science* **2007**, *317*, 41–42. [CrossRef]
5. Giri, C.; Ochieng, E.; Tieszen, L.L.; Zhu, Z.; Singh, A.; Loveland, T.; Masek, J.; Duke, N. Status and distribution of mangrove forests of the world using earth observation satellite data. *Glob. Ecol. Biogeogr.* **2011**, *20*, 154–159. [CrossRef]
6. Spalding, M. *World Atlas of Mangroves*, 1st ed.; Routledge: London, UK, 2010. [CrossRef]
7. Spalding, M.D.; Blasco, F.; Field, C.D. *World Mangrove Atlas*; The International Society for Mangrove Ecosystems: Okinawa, Japan, 1997; p. 178. Available online: http://www.archive.org/details/worldmangroveatl97spal (accessed on 1 April 2022).
8. Thomas, N.; Lucas, R.; Bunting, P.; Hardy, A.; Rosenqvist, A.; Simard, M. Distribution and drivers of global mangrove forest change, 1996–2010. *PLoS ONE* **2017**, *12*, e0179302. [CrossRef]
9. Valiela, I.; Bowen, J.L.; York, J.K. Mangrove forests: One of the world's threatened major tropical environments. *BioScience* **2001**, *51*, 807–815. [CrossRef]
10. Hamilton, S.E.; Casey, D. Creation of a high spatio-temporal resolution global database of continuous mangrove forest cover for the 21st century (CGMFC-21). *Glob. Ecol. Biogeogr.* **2016**, *25*, 729–738. [CrossRef]
11. Goldberg, L.; Lagomasino, D.; Thomas, N.; Fatoyinbo, T. Global declines in human-driven mangrove loss. *Glob. Chang. Biol.* **2020**, *26*, 5844–5855. [CrossRef]
12. Giri, C.; Long, J.; Abbas, S.; Murali, R.M.; Qamer, F.M.; Pengra, B.; Thau, D. Distribution and dynamics of mangrove forests of South Asia. *J. Environ. Manag.* **2015**, *148*, 101–111. [CrossRef]
13. Richards, D.R.; Friess, D.A. Rates and drivers of mangrove deforestation in Southeast Asia, 2000–2012. *Proc. Natl. Acad. Sci. USA* **2016**, *113*, 344–349. [CrossRef]
14. Giri, C.; Zhu, Z.; Tieszen, L.L.; Singh, A.; Gillette, S.; Kelmelis, J.A. Mangrove forest distributions and dynamics (1975–2005) of the tsunami-affected region of Asia. *J. Biogeogr.* **2008**, *35*, 519–528. [CrossRef]
15. Nordhaus, I.; Toben, M.; Fauziyah, A. Impact of deforestation on mangrove tree diversity, biomass and community dynamics in the Segara Anakan lagoon, Java, Indonesia: A ten-year perspective. *Estuar. Coast. Shelf Sci.* **2019**, *227*, 106300. [CrossRef]
16. Queiroz, L.D.; Rossi, S.; Calvet-Mir, L.; Ruiz-Mallen, I.; Garcia-Betorz, S.; Salva-Prat, J.; Meireles, A.J.D. Neglected ecosystem services: Highlighting the socio-cultural perception of mangroves in decision-making processes. *Ecosyst. Serv.* **2017**, *26*, 137–145. [CrossRef]

17. Lewis, R.R.; Milbrandt, E.C.; Brown, B.; Krauss, K.W.; Rovai, A.S.; Beever Iii, J.W.; Flynn, L.L. Stress in mangrove forests: Early detection and preemptive rehabilitation are essential for future successful worldwide mangrove forest management. *Mar. Pollut. Bull.* **2016**, *109*, 764–771. [CrossRef]
18. Proisy, C.; Viennois, G.; Sidik, F.; Andayani, A.; Enright, J.A.; Guitet, S.; Gusmawati, N.; Lemonnier, H.; Muthusankar, G.; Olagoke, A.; et al. Monitoring mangrove forests after aquaculture abandonment using time series of very high spatial resolution satellite images: A case study from the Perancak estuary, Bali, Indonesia. *Mar. Pollut. Bull.* **2018**, *131*, 61–71. [CrossRef]
19. Wang, L.; Jia, M.; Yin, D.; Tian, J. A review of remote sensing for mangrove forests: 1956–2018. *Remote Sens. Environ.* **2019**, *231*, 111223. [CrossRef]
20. Rahman, M.M.; Lagomasino, D.; Lee, S.; Fatoyinbo, T.; Ahmed, I.; Kanzaki, M. Improved assessment of mangrove forests in Sundarbans East Wildlife Sanctuary using WorldView 2 and TanDEM-X high resolution imagery. *Remote Sens. Ecol. Conserv.* **2019**, *5*, 136–149. [CrossRef]
21. Everitt, J.H.; Yang, C.; Sriharan, S.; Judd, F.W. Using High Resolution Satellite Imagery to Map Black Mangrove on the Texas Gulf Coast. *J. Coast. Res.* **2008**, *2008*, 1582–1586. [CrossRef]
22. Neukermans, G.; Dahdouh-Guebas, F.; Kairo, J.G.; Koedam, N. Mangrove species and stand mapping in Gazi bay (Kenya) using Quickbird satellite imagery. *J. Spat. Sci.* **2008**, *53*, 75–86. [CrossRef]
23. Lee, T.-M.; Yeh, H.-C. Applying remote sensing techniques to monitor shifting wetland vegetation: A case study of Danshui River estuary mangrove communities, Taiwan. *Ecol. Eng.* **2009**, *35*, 487–496. [CrossRef]
24. Wang, L.; Sousa, W.P.; Gong, P.; Biging, G.S. Comparison of IKONOS and QuickBird images for mapping mangrove species on the Caribbean coast of Panama. *Remote Sens. Environ.* **2004**, *91*, 432–440. [CrossRef]
25. Proisy, C.; Féret, J.-B.; Lauret, N.; Gastellu-Etchegorry, J.-P. (Eds.) *Mangrove Forest Dynamics Using Very High Spatial Resolution Optical Remote Sensing*; Elsevier: Paris, France, 2016; Volume 7, pp. 269–295. [CrossRef]
26. Proisy, C.; Couteron, P.; Fromard, F. Predicting and mapping mangrove biomass from canopy grain analysis using Fourier-based textural ordination of IKONOS images. *Remote Sens. Environ.* **2007**, *109*, 379–392. [CrossRef]
27. Taureau, F.; Robin, M.; Proisy, C.; Fromard, F.; Imbert, D.; Debaine, F. Mapping the Mangrove Forest Canopy Using Spectral Unmixing of Very High Spatial Resolution Satellite Images. *Remote Sens.* **2019**, *11*, 367. [CrossRef]
28. Wang, T.; Zhang, H.; Lin, H.; Fang, C. Textural–spectral feature-based species classification of mangroves in Mai Po Nature Reserve from Worldview-3 imagery. *Remote Sens.* **2016**, *8*, 24. [CrossRef]
29. Proisy, C.; Walcker, R.; Blanchard, E.; Gardel, A.; Anthony, E.J. (Eds.) *Mangroves: A Natural Early Warning System of Erosion on Open Muddy Coasts in French Guiana*; Elsevier: Amsterdam, The Netherlands, 2021; pp. 47–63. [CrossRef]
30. Gnanappazham, L.; Selvam, V. The dynamics in the distribution of mangrove forests in Pichavaram, South India—Perception by user community and remote sensing. *Geocarto Int.* **2011**, *26*, 475–490. [CrossRef]
31. Olwig, M.F.; Sørensen, M.K.; Rasmussen, M.S.; Danielsen, F.; Selvam, V.; Hansen, L.B.; Nyborg, L.; Vestergaard, K.B.; Parish, F.; Karunagaran, V.M. Using remote sensing to assess the protective role of coastal woody vegetation against tsunami waves. *Int. J. Remote Sens.* **2007**, *28*, 3153–3169. [CrossRef]
32. Selvam, V.; Ravichandran, K.K.; Gnanappazham, L.; Navamuniyammal, M. Assessment of community-based restoration of Pichavaram mangrove wetland using remote sensing data. *Curr. Sci.* **2003**, *85*, 794–798.
33. Vani, M.; Rama Chandra Prasad, P. (Eds.) *Geospatial Assessment of Spatio-Temporal Changes in Mangrove Vegetation of Pichavaram Region, Tamil Nadu, India*; Springer International Publishing: Cham, Switzerland, 2018; pp. 89–102. [CrossRef]
34. Löf, M.; Madsen, P.; Metslaid, M.; Witzell, J.; Jacobs, D.F. Restoring forests: Regeneration and ecosystem function for the future. *New For.* **2019**, *50*, 139–151. [CrossRef]
35. Beck, H.E.; Zimmermann, N.E.; McVicar, T.R.; Vergopolan, N.; Berg, A.; Wood, E.F. Present and future Köppen-Geiger climate classification maps at 1-km resolution. *Sci. Data* **2018**, *5*, 180214. [CrossRef]
36. Selvam, V.; Ravichandaran, K.K.; Karunakaran, V.M.; Mani, K.G.; Beula, E.J.; Gnanappazham, L. *Pichavaram Mangrove Wetland: Situation Analysis*; MS Swaminathan Research Foundation: Chennai, India, 2010; p. 39.
37. Sathyanathan, R.; Thattai, D.; Selvam, V. The Coleroon river flow and its effect on the Pichavaram mangrove ecosystem. *J. Coast. Conserv.* **2014**, *18*, 309–322. [CrossRef]
38. Kathiresan, K. A review of studies on Pichavaram mangrove, southeast India. *Hydrobiologia* **2000**, *430*, 185–205. [CrossRef]
39. Sathya, T.; Sekar, C. Stakeholder Preference, Dependence and Attitude towards Conservation of Mangrove Eco-System in South-East Coast of India. *Innovare J. Soc. Sci.* **2014**, *2*, 15–25.
40. Kuester, M.A. Absolute Radiometric Calibration: 2016 v0, Digital Globe. 2017. Available online: https://dgv4-cms-production.s3.amazonaws.com/uploads/document/file/136/ABSRADCAL_FLEET_2016v0_Rel20170606.pdf (accessed on 1 April 2022).
41. Wilkinson, G.G. Results and implications of a study of fifteen years of satellite image classification experiments. *IEEE Trans. Geosci. Remote Sens.* **2005**, *43*, 433–440. [CrossRef]
42. Kathiresan, K. Globally threatened mangrove species in India. *Curr. Sci.* **2010**, *98*, 1551.
43. Kathiresan, K.; Rajendran, N. Fishery resources and economic gain in three mangrove areas on the south-east coast of India. *Fish. Manag. Ecol.* **2002**, *9*, 277–283. [CrossRef]
44. Viennois, G.; Proisy, C.; Féret, J.-B.; Prosperi, J.; Sidik, F.; Suhardjono; Rahmania, R.; Longépé, N.; Germain, O.; Gaspar, P. Multitemporal analysis of high spatial resolution satellite imagery for mangrove species mapping, Bali, Indonesia. *IEEE J. Sel. Top. Appl. Earth Observ. Remote Sens.* **2016**, *9*, 3680–3686. [CrossRef]

45. Unnikrishnan, A.S.; Nidheesh, A.G.; Lengaigne, M. Sea-level-rise trends off the Indian coasts during the last two decades. *Curr. Sci.* **2015**, *108*, 966–971.
46. Jayanthi, M.; Thirumurthy, S.; Nagaraj, G.; Muralidhar, M.; Ravichandran, P. Spatial and temporal changes in mangrove cover across the protected and unprotected forests of India. *Estuar. Coast. Shelf Sci.* **2018**, *213*, 81–91. [CrossRef]
47. Senthalir, S. Shrimp Farms Threatening Pichavaram Forest. *The Hindu*. 9 August 2017. Available online: https://www.thehindu.com/news/cities/puducherry/shrimp-farms-threatening-pichavaram-forest/article19453172.ece (accessed on 1 April 2022).
48. Srivastava, J.; Farooqui, A.; Hussain, S.M. Vegetation history and salinity gradient during the last 3700 years in Pichavaram estuary, India. *J. Earth Syst. Sci.* **2012**, *121*, 1229–1237. [CrossRef]
49. Bosire, J.O.; Dahdouh-Guebas, F.; Walton, M.; Crona, B.I.; Lewis III, R.R.; Field, C.; Kairo, J.G.; Koedam, N. Functionality of restored mangroves: A review. *Aquat. Bot.* **2008**, *89*, 251–259. [CrossRef]
50. Kamali, B.; Hashim, R. Mangrove restoration without planting. *Ecol. Eng.* **2011**, *37*, 387–391. [CrossRef]
51. Rossi, R.E.; Archer, S.K.; Giri, C.; Layman, C.A. The role of multiple stressors in a dwarf red mangrove (*Rhizophora mangle*) dieback. *Estuar. Coast. Shelf Sci.* **2020**, *237*, 106660. [CrossRef]
52. Lagomasino, D.; Fatoyinbo, T.; Castañeda-Moya, E.; Cook, B.D.; Montesano, P.M.; Neigh, C.S.R.; Corp, L.A.; Ott, L.E.; Chavez, S.; Morton, D.C. Storm surge and ponding explain mangrove dieback in southwest Florida following Hurricane Irma. *Nat. Commun.* **2021**, *12*, 4003. [CrossRef] [PubMed]
53. Servino, R.N.; Gomes, L.E.d.O.; Bernardino, A.F. Extreme weather impacts on tropical mangrove forests in the Eastern Brazil Marine Ecoregion. *Sci. Total Environ.* **2018**, *628–629*, 233–240. [CrossRef]
54. Sippo, J.Z.; Santos, I.R.; Sanders, C.J.; Gadd, P.; Hua, Q.; Lovelock, C.E.; Santini, N.S.; Johnston, S.G.; Harada, Y.; Reithmeir, G.; et al. Reconstructing extreme climatic and geochemical conditions during the largest natural mangrove dieback on record. *Biogeosciences* **2020**, *17*, 4707–4726. [CrossRef]
55. Lovelock, C.E.; Feller, I.C.; Reef, R.; Hickey, S.; Ball, M.C. Mangrove dieback during fluctuating sea levels. *Sci. Rep.* **2017**, *7*, 1680. [CrossRef]
56. Duke, N.C.; Kovacs, J.M.; Griffiths, A.D.; Preece, L.; Hill, D.J.E.; van Oosterzee, P.; Mackenzie, J.; Morning, H.S.; Burrows, D. Large-scale dieback of mangroves in Australia's Gulf of Carpentaria: A severe ecosystem response, coincidental with an unusually extreme weather event. *Mar. Freshw. Res.* **2017**, *68*, 1816–1829. [CrossRef]
57. Duke, N.C.; Bell, A.M.; Pederson, D.K.; Roelfsema, C.M.; Bengtson Nash, S. Herbicides implicated as the cause of severe mangrove dieback in the Mackay region, NE Australia: Consequences for marine plant habitats of the GBR World Heritage Area. *Mar. Pollut Bull.* **2005**, *51*, 308–324. [CrossRef]
58. Mathevet, R.; Targowla, S.; Munisamy, A.; Govindan, V.; Narayanan, A.; Bautès, N. Wetlands for a sustainable urban future: Insights from Pondicherry, South India. *Grassroots J. Nat. Resour.* **2020**, *3*, 74–93. [CrossRef]
59. Prasad, S. Hunt for Hydrocarbons Could Sink Pichavaram, Fear Activists. *The Hindu*. 13 June 2019. Available online: https://www.thehindu.com/news/cities/puducherry/hunt-for-hydrocarbons-could-sink-pichavaram-fear-activists/article27891952.ece (accessed on 1 April 2022).
60. Mathevet, R.; Poulin, B. From conservation biology to conservation geography. *Bull. L'assoc. Géogr. Fr.* **2006**, *83*, 341–354. [CrossRef]